Topological rejection of noise by quantum skyrmions: Supplementary Information

Pedro Ornelas,[1] Isaac Nape,[1] Robert de Mello Koch,[2,3] and Andrew Forbes[1]

[1]*School of Physics, University of the Witwatersrand, Private Bag 3, Wits 2050, South Africa*
[2]*School of Science, Huzhou University, Huzhou 313000, China*
[3]*Mandelstam Institute for Theoretical Physics, School of Physics, University of the Witwatersrand, Private Bag 3, Wits 2050, South Africa*

I. FORMULATION OF NON-LOCAL QUANTUM SKYRMION

A pure non-local biphoton hybrid entangled state of two photons, A and B, correlated in OAM-Polarization (as depicted in Fig. S1 (a)), can in general be written in the form

$$|\Psi\rangle = \frac{1}{\sqrt{2}}\left(|\ell_1\rangle_A |P_1\rangle_B + e^{i\delta}|\ell_2\rangle_A |P_2\rangle_B\right), \quad \text{(S.1)}$$

where ℓ_1 and ℓ_2 denote OAM of $\ell_1\hbar$ and $\ell_2\hbar$ per photon, respectively, and $|P_1\rangle, |P_2\rangle$ are orthogonal polarization states, while δ allows for a relative phase between the two components of the state vector. Photon A's states live on the Hilbert space $\mathcal{H}_A$ spanned by the states $\{|\ell_1\rangle, |\ell_2\rangle\}$ and photon B's states live on the Hilbert space $\mathcal{H}_B$ spanned by the states $\{|P_1\rangle, |P_2\rangle\}$. $|\Psi\rangle$ belongs to the Hilbert space $\mathcal{H} = \mathcal{H}_A \otimes \mathcal{H}_B$. For states with $|\ell_1| \neq |\ell_2|$ it has been shown that the correlations between these photons form the desired skyrmionic mapping from $\mathcal{S}^2 \to \mathcal{S}^2$ (equivalent to the mapping $\mathcal{R}^2 \to \mathcal{S}^2$ through a stereographic projection of the spatial $\mathcal{S}^2$ to the real plane $\mathcal{R}^2$) as depicted in Fig. S1 (b) [1]. Expressing photon A in position basis, using $|\ell\rangle = \int_{\mathcal{R}^2} |\mathrm{LG}_\ell(\mathbf{r})|e^{i\ell\phi}|\mathbf{r}\rangle d^2r$ where $\mathrm{LG}_\ell(\mathbf{r})$ are the Laguerre-Gaussian fields and $|\mathbf{r}\rangle$ are position states, we find

$$|\Psi\rangle = \int_{\mathcal{R}^2} |\mathbf{r}\rangle_A \left(a(\mathbf{r}_A)|P_1\rangle_B + b(\mathbf{r}_A)|P_2\rangle_B\right) d^2r_A, \quad \text{(S.2)}$$

where $a(\mathbf{r}_A) \equiv |\mathrm{LG}_{\ell_1}(\mathbf{r}_A)|$, $b(\mathbf{r}_A) \equiv e^{i\Theta(\phi_A)}|\mathrm{LG}_{\ell_2}(\mathbf{r}_A)|$, $\Theta(\phi_A) = \Delta\ell\phi_A + \delta$ and $\Delta\ell = \ell_2 - \ell_1$. In this formulation, it can be deduced that a spatial measurement on photon A, collapses photon B into a particular polarization state as shown in Fig. S1 (b). For a non-trivial skyrmionic topology, we have that a full set of spatial measurements on photon A collapses photon B into every possible polarization state as depicted in Fig. S1 (c). This non-local topology can be depicted compactly by combining the spatial sphere and polarization states together as shown in Fig. S1 (c) where the tail of each polarization state vector for photon B is adjacent to its correlated position in photon A.

The Skyrmion number of these states can then be calculated using the equation $N = \frac{1}{4\pi}\int_{\mathcal{R}^2} \Sigma_z(x,y)dxdy$ [2] where $\Sigma_z(x,y) = \epsilon_{pqr} S_p \frac{\partial S_q}{\partial x}\frac{\partial S_r}{\partial y}$ and ϵ_{pqr} is the Levi-Civita symbol. The integral in the Skyrmion number calculation computes the surface area of photon B's parameter space covered by the mapping defined by the wavefunction given in Eqn. S.2. Thus, since the parameter space is a unit sphere, dividing by the surface area of the sphere (4π), we find the wrapping number N of the non-local topology.

The quantum Stokes parameters, S_i, are given by the expectation values of the Pauli matrices, which are calculated by taking the diagonal matrix element at position $\mathbf{r}$ for photon A and the partial trace over photon B, such that $S_i = \mathrm{Tr}_B(\langle|\mathbf{r}\rangle_A {}_A\langle\mathbf{r}| \otimes \sigma_{B,i}\rangle) = \mathrm{Tr}_B(\sigma_{B,i}\ {}_A\langle\mathbf{r}|\Psi\rangle\langle\Psi|\mathbf{r}\rangle_A)$. From this it can be shown that the Skyrmion number depends on the difference between ℓ_1 and ℓ_2, according to $N = m\Delta\ell$ with $m = \mathrm{sign}(|\ell_1| - |\ell_2|)$[2–5]. The value of $\Delta\ell$ known as the vorticity controls the magnitude of the Skyrmion number and can be used to switch between Skyrmions ($m = 1$) and anti-Skyrmions ($m = -1$). It should be noted that while we are studying states with integer topological numbers of mappings between spheres, the existence of meron structures with half-integer topological numbers have been studied in classical vectorial fields [6, 7] albeit these structures are strictly not skyrmions as they do not arise from maps between spheres. Furthermore, while the chosen polarization basis and the helicity, δ, play no role in determining the topology of the state it can be used to switch between different textures. Conventionally, Skyrmions are defined in the $|R\rangle, |L\rangle$ polarization basis, $S_z = S_3$, with Bimerons defined under an arbitrary choice of polarization basis [5] (see Ref. [8] for a discussion on the topic). However, we are free to perform a rotation of the Poincaré sphere which does not alter the topology of our states such that we can instead consider Skyrmions defined in the $|H\rangle, |V\rangle$ polarization basis, $S_z = S_1$, following the convention we used in our previous work [1]. Furthermore, we can also switch between different textures by changing δ, for example if $N = 1$ and $\delta = 0, \pi$ we have a Neél-type Skyrmion, and if $\delta = \pm\frac{\pi}{2}$ we have a Bloch-type Skyrmion. We note that the state could have been expressed in a different basis, such as momentum. However, this would incur a significant computational penalty, as the Fourier transforms required implies that our Skyrmion number calculation would become a complicated double convolution of the Fourier transform of the Stokes parameter. Therefore the continuous position basis is not only more intuitive, it is computationally less cumbersome.

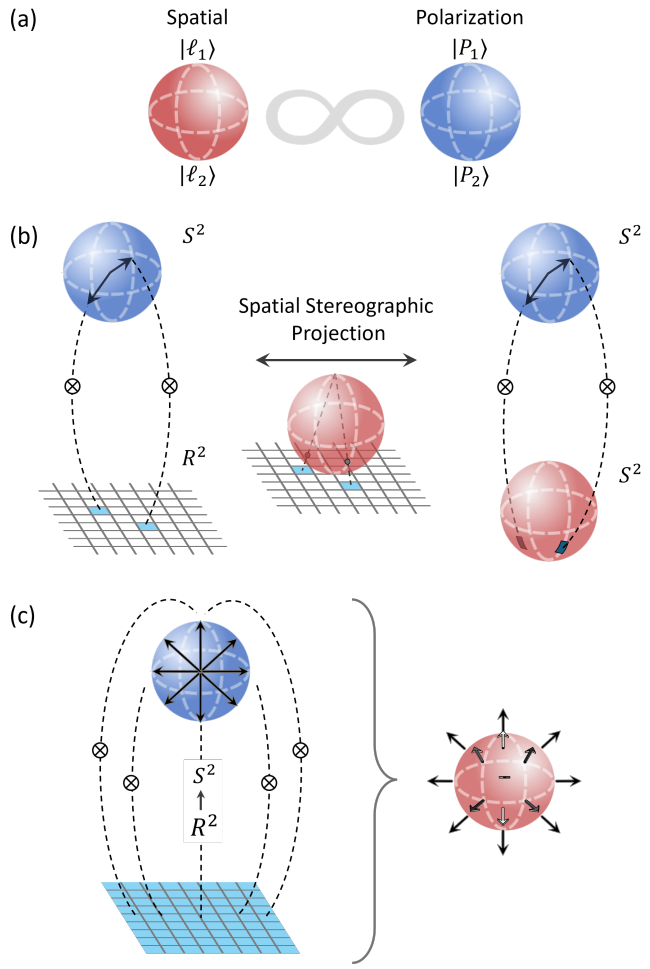

FIG. S1: (a) Hybrid entangled state of photons A and B which share OAM-polarization correlations. (b) Such a state also yields position-polarization correlations where a position measurement on photon A yields in coincidence a polarization state collapse for photon B. Through a stereographic projection, this can also be seen as a mapping between a spatial sphere and a polarization sphere. (c) Observation of photon B's state in coincidence with spatial measurements performed on photon A reveals the non-local skyrmionic structure embedded within the entangled state. The topological structure can be compactly represented by combining the spatial sphere of photon A and the polarization state vectors of photon B whose tail is adjacent to its correlated position in photon A.

II. QUANTUM TOPOLOGICAL INVARIANCE TO ISOTROPIC NOISE

We now consider subjecting our state, $|\Psi\rangle$, to environmental/ "white" noise, according to the isotropic model where the purity of the state is degraded by mixing it with a maximally mixed state according to

$$\rho = p\,|\Psi\rangle\langle\Psi| + \frac{1-p}{d^2}\mathbb{1}_{d^2}, \tag{S.3}$$

where $d = 2$, $p \in [0,1]$ is a parameter controlling the degree of purity of the state with $p = 1$ giving a pure state ($|\Psi\rangle\langle\Psi|$) and $p = 0$ giving a maximally mixed state ($\frac{1}{d^2}\mathbb{1}_{d^2}$) and $\mathbb{1}_{d^2}$, the $d^2 \times d^2$ identity matrix, is the identity operator on $\mathcal{H}$. The purity, γ, of a state is given by $\mathrm{Tr}(\rho^2)$. It follows that γ is related to p according to

$$\begin{aligned}
\gamma &= \mathrm{Tr}\left(\left(p\,|\Psi\rangle\langle\Psi| + \frac{1-p}{d^2}\mathbb{1}_{d^2}\right)^2\right) \\
&= \mathrm{Tr}\left(p^2\,|\Psi\rangle\langle\Psi| + 2p\frac{(1-p)}{d^2}\,|\Psi\rangle\langle\Psi| + \frac{(1-p)^2}{d^4}\mathbb{1}_{d^2}\right) \\
&= p^2 + 2p\frac{(1-p)}{d^2} + \frac{(1-p)^2}{d^2} \\
&= p^2 + \frac{1-p^2}{d^2}.
\end{aligned} \tag{S.4}$$

To calculate the Skyrmion number we must consider how the quantum Stokes parameters are affected by the isotropic noise with the model given above,

$$\begin{aligned}
S_i' &= \mathrm{Tr}_B\left(\sigma_{B,i}\,{}_A\langle\mathbf{r}|\rho|\mathbf{r}\rangle_A\right) \\
&= \mathrm{Tr}_B\Big(\sigma_{B,i}\big(p\,{}_A\langle\mathbf{r}|\Psi\rangle\langle\Psi|\mathbf{r}\rangle_A \\
&\qquad + \frac{1-p}{4}\,{}_A\langle\mathbf{r}|\mathbb{1}_4|\mathbf{r}\rangle_A\big)\Big)
\end{aligned} \tag{S.5}$$

It should be noted that without loss of generality we have chosen to restrict ourselves to the original 2D OAM hilbert space of photon A, by projecting onto only that hilbert space. This is because isotropic noise treats every OAM state in the exact same way (mixing it with the identity), thus we are justified in only considering states within which we start with a non-zero signal contribution. To compute the diagonal matrix element of $\mathbb{1}_4$, start by noting that we have

$$a(\mathbf{r}) = \langle\mathbf{r}|\ell_1\rangle \qquad b(\mathbf{r}) = \langle\mathbf{r}|\ell_2\rangle \tag{S.6}$$

which follow by comparing (S.1) and (S.2). We note that we have ignored the factor $\frac{1}{\sqrt{2}}$ in (S.6) since to obtain correctly normalized quantum Stokes parameters, we must choose

$$|a|^2 + |b|^2 = 1 \tag{S.7}$$

at all $\mathbf{r}$. Using

$$\begin{aligned}
\mathbb{1}_4 &= |\ell_1\rangle_A|P_1\rangle_B\,{}_A\langle\ell_1|\,{}_B\langle P_1| + |\ell_1\rangle_A|P_2\rangle_B\,{}_A\langle\ell_1|\,{}_B\langle P_2| \\
&\quad + |\ell_2\rangle_A|P_1\rangle_B\,{}_A\langle\ell_2|\,{}_B\langle P_1| + |\ell_2\rangle_A|P_2\rangle_B\,{}_A\langle\ell_2|\,{}_B\langle P_2|
\end{aligned}$$

we easily find (use (S.6) and (S.7))

$$\begin{aligned}
\langle\mathbf{r}|\mathbb{1}_4|\mathbf{r}\rangle &= 2|a|^2|P_1\rangle_B\,{}_B\langle P_1| + 2|a|^2|P_2\rangle_B\,{}_B\langle P_2| \\
&\quad + 2|b|^2|P_1\rangle_B\,{}_B\langle P_1| + 2|b|^2|P_2\rangle_B\,{}_B\langle P_2| \\
&= 2\mathbb{1}_2
\end{aligned}$$

where $\mathbb{1}_2$ is the identity operator on $\mathcal{H}_B$ and $a \equiv a(\mathbf{r})$ and $b \equiv b(\mathbf{r})$. Consequently we have

$$S_i' = \mathrm{Tr}_B\Big(\sigma_{B,i}\big(p\,{}_A\langle\mathbf{r}|\Psi\rangle\langle\Psi|\mathbf{r}\rangle_A + \frac{1-p}{2}\mathbb{1}_2\big)\Big) \tag{S.8}$$

It is satisfying that after taking the diagonal matrix element, the maximally mixed state in $\mathcal{H}$ has been replaced by the maximally mixed state in $\mathcal{H}_B$. Using the linearity of the trace operation and the fact that the Pauli matrices are traceless, we have

$$\begin{aligned} S_i' &= p\mathrm{Tr}_B\left(\sigma_{B,i}\ {}_A\langle \mathbf{r}|\Psi\rangle\langle\Psi|\mathbf{r}\rangle_A\right) \\ &\quad + \frac{1-p}{2}\mathrm{Tr}_B\left(\sigma_{B,i}\right) \\ &= p\,\mathrm{Tr}_B\left(\sigma_{B,i}\ {}_A\langle \mathbf{r}|\Psi\rangle\langle\Psi|\mathbf{r}\rangle_A\right) \\ &= pS_i \end{aligned} \tag{S.9}$$

where S_i are the quantum Stokes parameters for the pure state without isotropic noise. Therefore, the effect of isotropic noise on the state is to multiply the Stokes parameters, S_i, by a constant factor p. The Skyrmion number assumes normalization such that $\Sigma_i^3 S_i^2 = 1$. After correct normalization of the Stokes parameters this constant p factor does not contribute demonstrating that isotropic noise does not alter the topology. This demonstrates that the skyrmionic topology of the state is invariant to isotropic noise as long as a portion of the pure state survives i.e., $p > 0$ or equivalently $\gamma > \frac{1}{d^2}$.

III. REJECTION MECHANISM UNDERLYING PROJECTIVE MEASUREMENTS

To further clarify the result obtained in the previous section, we will now argue that the invariance of the skyrmionic topology to isotropic noise can be understood as noise rejection by projective measurements made on our state. Towards this end we employ the spectral decomposition of the Pauli matrices, $\sigma_{B,i} = \lambda_i^+ P_i^+ + \lambda_i^- P_i^-$ where $P_i^\pm = |\lambda_i^\pm\rangle\langle\lambda_i^\pm|$ and the eigenvalues are $\lambda_i^\pm = \pm 1$. Substituting this into Eqn. S.9 we find

$$\begin{aligned} S_i' &= \mathrm{Tr}_B\left(P_i^+\left[p\ {}_A\langle \mathbf{r}|\Psi\rangle\langle\Psi|\mathbf{r}\rangle_A + \frac{1-p}{2}\mathbb{1}_2\right]\right) \\ &\quad -\mathrm{Tr}_B\left(P_i^-\left[p\ {}_A\langle \mathbf{r}|\Psi\rangle\langle\Psi|\mathbf{r}\rangle_A + \frac{1-p}{2}\mathbb{1}_2\right]\right) \\ &= (I_{i,\mathrm{pure}}^+ + I_{i,\mathrm{noise}}^+) - (I_{i,\mathrm{pure}}^- + I_{i,\mathrm{noise}}^-), \end{aligned} \tag{S.10}$$

where $I_{i,\mathrm{pure}}^\pm = \mathrm{Tr}_B\left(P_i^\pm p\ {}_A\langle \mathbf{r}|\Psi\rangle\langle\Psi|\mathbf{r}\rangle_A\right)$ and $I_{i,\mathrm{noise}}^\pm = \mathrm{Tr}_B\left(P_i^\pm \frac{1-p}{2}\mathbb{1}_2\right)$. Experimentally, we measure the quantities $I_{i,\mathrm{exp}}^+ = I_{i,\mathrm{pure}}^+ + I_{i,\mathrm{noise}}^+$ and $I_{i,\mathrm{exp}}^- = I_{i,\mathrm{pure}}^- + I_{i,\mathrm{noise}}^-$. Since the eigenvalues of the Pauli matrices are non-degenerate we have that $\mathrm{Tr}\left(P_i^+\right) = \mathrm{Tr}\left(P_i^-\right) = 1$. Therefore $I_{i,\mathrm{noise}}^+ = I_{i,\mathrm{noise}}^-$, so that $S_i' = I_{i,\mathrm{exp}}^+ - I_{i,\mathrm{exp}}^- = I_{i,\mathrm{pure}}^+ - I_{i,\mathrm{pure}}^+$. This shows that each pair of projective measurements required to calculate each Pauli observable, receive identical noise contributions, which thus cancels in their difference, explaining the noise rejection.

IV. EXPERIMENT

A schematic of the experiment conducted is shown in Fig. S2. Entangled photon pairs were generated through spontaneous parametric down-conversion (SPDC), where a 355 nm wavelength, collimated Gaussian beam was sent through a 3 mm long, Type-I Barium Borate (BBO) nonlinear crystal (NC). A band-pass filter (BPF) centred at 710 nm wavelength was used to filter out the unconverted pump beam. From the SPDC process, the generated photons were correlated in OAM, sharing the non-separable state, $|\Psi\rangle = \Sigma_\ell c_\ell |\ell\rangle_A \otimes |-\ell\rangle_B$, where the coefficients, c_ℓ, determined the weightings for each subspace that was spanned by the OAM eigenstates, $|\pm\ell\rangle$, for each photon. The two entangled photons (photon A and B) were then spatially separated using a 50:50 beam-splitter (BS). In order to prepare the desired non-local skyrmionic state the initial OAM-OAM entangled state was mapped to an arbitrary hybrid entangled state of the form

$$|\Psi\rangle = \frac{1}{\sqrt{2}}\left(|\ell_1\rangle_A|H\rangle_B + |\ell_2\rangle_A|V\rangle_B\right), \tag{S.11}$$

through the use of a digital spatial-to-polarization coupling (SPC) approach [9] where the spatial information of photon B was coupled to polarization. To achieve the desired arbitrary state given in Eq. S.11, the OAM DOF of photon B was coupled to orthogonal polarization states using a post-selection of the desired OAM subspace with separate modulations by an SLM. The transformations undergone by the state of photon B due to the entire SPC can be broken down as follows (we ignore contributions from states which will not couple into the fibre, i.e we only consider $|m\rangle = |0\rangle$) $|H,\ell_1'\rangle + |V,\ell_2'\rangle \xrightarrow{\mathrm{SLM}} |H,\ell_1'+\ell_1\rangle + |V,\ell_2'\rangle \xrightarrow{\mathrm{QWP}} |L,\ell_1'+\ell_1\rangle + |R,\ell_2'\rangle \xrightarrow{\mathrm{M}} |R,\ell_1'+\ell_1\rangle + |L,\ell_2'\rangle \xrightarrow{\mathrm{QWP}} |V,\ell_1'+\ell_1\rangle + |H,\ell_2'\rangle \xrightarrow{\mathrm{SLM}} |V,\ell_1'+\ell_1\rangle + |H,\ell_2'+\ell_2\rangle$, where coupling into the fibre ensures that $\ell_1 = -\ell_1'$ and $\ell_2 = -\ell_2'$ thereby erasing the OAM information from photon B as it becomes a separable DOF in photon B. It is clear then that the desired OAM subspace, $\{\ell_1, \ell_2\}$ is selected by displaying those modes on the SLM. Following the state preparation, spatially separated projective measurements were performed on both photons and they were observed in coincidence allowing for the construction of a full quantum state tomography of the biphoton state. Photon A was detected through a coupled detection system consisting of an SLM and SMF coupled to an avalanche photon detector (APD). Photon B was measured using a set of polarization optics, a HWP orientated to 45° and a linear polarizer (LP) orientated at 90°.

To identify the highest-order topological state achievable in the experiment, we must first identify the highest OAM state achievable. We conducted an OAM spiral bandwidth measurement, which yielded a Schmidt mode number of $K = 11$. This result indicates that the highest-order OAM state that can be reliably measured in the experiment is $\ell = \pm 5$. However, due to losses introduced by

the optics in the SPC technique this was further reduced to $\ell = \pm 3$. We have provided experimental evidence for the resilience of states with topological number up to $N = 3$ (using OAM basis states $|0\rangle, |\ell\rangle, \ell \neq 0$ with OAM values from -3 to 3), which means that we were able to produce 6 states with distinct topological features. That being said it would be possible within the current configuration to exceed $|N| = 3$ as we can use the OAM values $\ell = -2, 3$ and $\ell = 2, -3$ to reach an upper value of $|N| = 5$. Beyond this higher order topological numbers can be achieved by improving the efficiency of the SPDC process, the SPC and the detection of higher-order OAM values.

Lastly, to vary the degree of isotropic noise in the experiment, a variable white light source was introduced whilst keeping the configuration of the rest of the experiment the same as discussed above. The white light source was characterized (See Fig. 4 in the main text) on the basis of how it affected the quantum contrast or state purity of the state (discussed in more detail in the next section). Therefore, we expect our model and experiment to remain agnostic to the origin of the noise whether that be the entanglement source, the detectors or the channel.

V. PURITY AND QUANTUM CONTRAST

The purity of the states generated within the experiment can directly be controlled by controlling the quantum contrast. The discussion that follows is based on the supplementary material given in reference [10].

Using the result given by Eq. S.4 it is clear that the purity of a state is dependent on the ratio between the signal and isotropic noise component of the state, p. This can directly be attributed to the quantum contrast Q_c of the state, which gives the ratio between the accidental and two-photon coincidences. This allows a relation between the probability p and Q_c as follows

$$Q_c = \frac{1 - p + pd}{1 - p} \implies p = \frac{Q_c - 1}{Q_c - 1 + d} \tag{S.12}$$

where d is the dimensionality of the state. Substituting Eq. S.4 and solving for γ then gives

$$\gamma = \frac{d\big(Q_c^2 - 2Q_c + 2\big) + 2(Q_c - 1)}{d(d + Q_c - 1)^2}. \tag{S.13}$$

Experimentally a full quantum state tomography is performed, consisting of 36 projective measurements (for $d = 2$) each with its own Q_c. When computing the Q_c for a state, the average Q_c across all 36 measurements is used. Furthermore, the Q_c is directly computed from the accidental coincidences and two photon coincidences according to

$$Q_c = \frac{1}{T}\frac{C}{AB} \tag{S.14}$$

where C is the two photon coincidences and $N_{acc} = TAB$ is the accidental coincidences with T being the coincidence window and A, B being the number of single photon detection events detected by the APDs in the optical path of photon A and B, respectively. With this in mind, the Q_c value used in Eq. S.13 is given by

$$Q_c = \frac{1}{36T}\sum_{i,j=1}^{6}\frac{C_{i.j}}{A_{i.j}B_{i.j}} \tag{S.15}$$

where the indices i, j reference a particular projective measurement used to build the full QST.

VI. CONCURRENCE AND FIDELITY

Beyond purity, quantities such as Concurrence and Fidelity also serve as entanglement witnesses for our states.

The fidelity was used to analytically compare our measured partially mixed states, ρ against an initial pure state $\rho_T = |\Psi\rangle\langle\Psi|$

$$F = \left(\mathrm{Tr}\left(\sqrt{\sqrt{\rho_T}\rho\sqrt{\rho_T}}\right)\right)^2, \tag{S.16}$$

The fidelity is 0 if the states are not identical or 1 when they are identical up to a global phase. However, since ρ is a partially mixed state, we find that when ρ becomes completely mixed, that is $\rho = \frac{1}{4}\mathbb{1}_{d^2}$, then $F = \frac{1}{4}$.

The concurrence was used to measure the degree of entanglement between the hybrid entangled photons. It was measured from

$$C(\rho) = \max\{0, \lambda_1 - \lambda_2 - \lambda_3 - \lambda_4\}, \tag{S.17}$$

where λ_i are eigenvalues of the operator $R = \mathrm{Tr}\left(\sqrt{\sqrt{\rho}\tilde{\rho}\sqrt{\rho}}\right)$ in descending order and $\tilde{\rho} = \sigma_y \otimes \sigma_y \rho^* \sigma_y \otimes \sigma_y$. The concurrence ranges from 0 for separable and completely mixed states to 1 for entangled states.

[1] P. Ornelas, I. Nape, R. de Mello Koch, and A. Forbes, "Non-local skyrmions as topologically resilient quantum entangled states of light," *Nature Photonics*, pp. 1–9, 2024.

[2] S. Gao, F. C. Speirits, F. Castellucci, S. Franke-Arnold, S. M. Barnett, and J. B. Götte, "Paraxial skyrmionic beams," *Physical Review A*, vol. 102, no. 5, p. 053513, 2020.

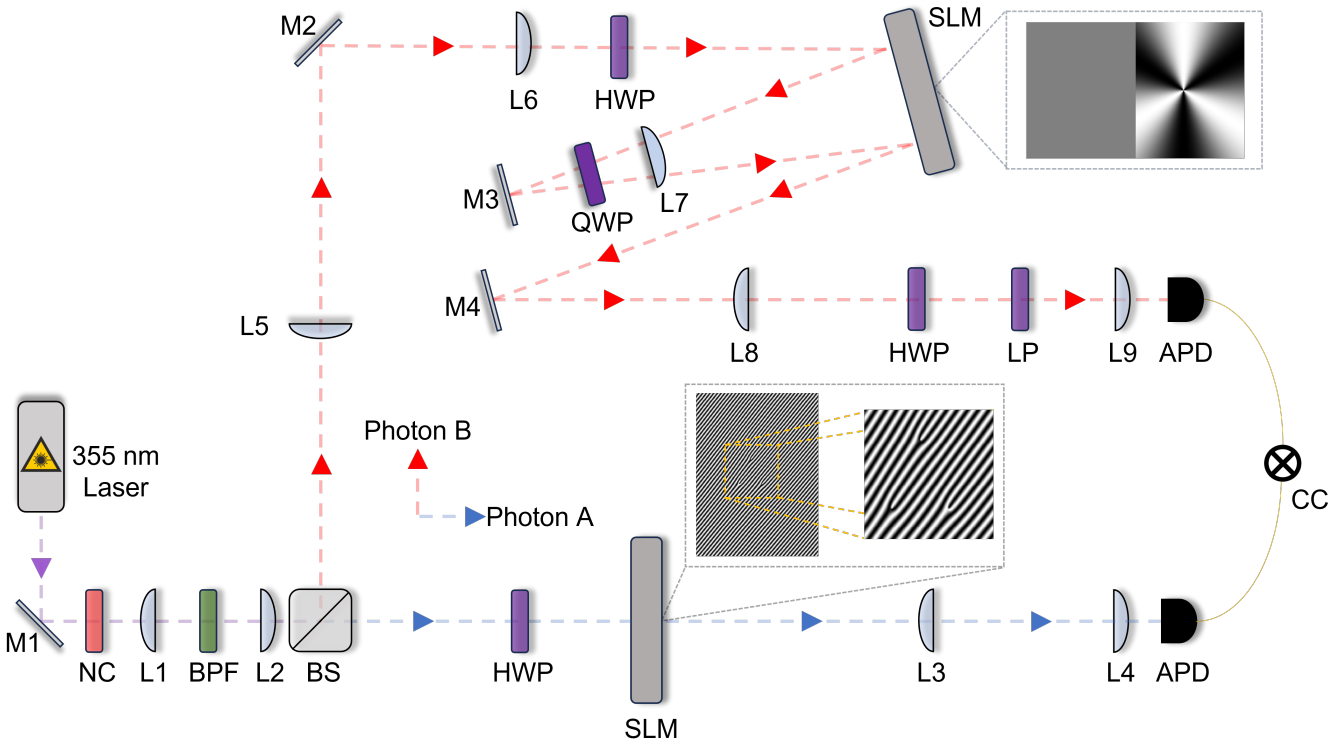

FIG. S2: Experimental setup for the generation and detection of non-local skyrmionic states. Some abbreviations: mirror (M), non-linear crystal (NC), lens (L), band-pass filter (BPF), 50:50 beam splitter (BS), half-wave plate (HWP), spatial light modulator (SLM), quarter-wave plate (QWP), linear polarizer (LP), avalanche photodiode (APD), coincidence counter (CC).

[3] H. Kuratsuji and S. Tsuchida, "Evolution of the stokes parameters, polarization singularities, and optical skyrmion," *Physical Review A*, vol. 103, no. 8, p. 023514, 2021.

[4] Y. Shen, E. C. Martínez, and C. Rosales-Guzmán, "Generation of optical skyrmions with tunable topological textures," *ACS Photonics*, vol. 9, no. 1, pp. 296–303, 2022.

[5] Y. Shen, "Topological bimeronic beams," *Optics Letters*, vol. 46, no. 15, pp. 3737–3740, 2021.

[6] D. Marco, I. Herrera, S. Brasselet, and M. A. Alonso, "Propagation-invariant optical meron lattices," *ACS Photonics*, 2024.

[7] K. Y. Bliokh, A. Niv, V. Kleiner, and E. Hasman, "Singular polarimetry: Evolution of polarization singularities in electromagnetic waves propagating in a weakly anisotropic medium," *Optics express*, vol. 16, no. 2, pp. 695–709, 2008.

[8] J. Chen, A. Forbes, and C.-W. Qiu, "More than just a name? from magnetic to optical skyrmions and the topology of light," *Light: Science & Applications*, vol. 14, no. 1, p. 28, 2025.

[9] I. Nape, A. G. de Oliveira, D. Slabbert, N. Bornman, J. Francis, P. H. S. Ribeiro, and A. Forbes, "An all-digital approach for versatile hybrid entanglement generation," *Journal of Optics*, vol. 24, p. 054003, mar 2022.

[10] F. Zhu, M. Tyler, N. H. Valencia, M. Malik, and J. Leach, "Is high-dimensional photonic entanglement robust to noise?," *AVS Quantum Science*, vol. 3, no. 1, p. 011401, 2021.